Journal of Applied Polymer Science

Aging Behavior and Mechanism of Bio-Based Engineering Polyester Elastomer Nanocomposites

Bowen Fang,[1] Hailan Kang,[1] Runguo Wang,[1] Zhao Wang,[1] Wencai Wang,[1] Liqun Zhang[1,2]

[1]State Key Laboratory of Organic–Inorganic Composites, Beijing University of Chemical Technology, Beijing 100029, People's Republic of China

[2]Key Laboratory of Beijing City on Preparation and Processing of Novel Polymer Materials, Beijing University of Chemical Technology, Beijing 100029, People's Republic of China

Correspondence to: L. Zhang (E-mail: zhanglq@mail.buct.edu.cn)

ABSTRACT: Bio-based elastomers used in industry have attracted much attention. We prepared bio-based engineering polyester elastomer (BEE) nanocomposites by mixing bio-based engineering polyester elastomers with carbon (CB). The CB/BEE nanocomposites were exposed to an artificial weathering environment for different time periods. Both its aging behavior changes and aging mechanism were investigated in this article. The tensile strength retention rates were each above 90% after aging at 100°C and 125°C for 72 h. CB/BEE nanocomposites exhibited good anti-aging properties. Furthermore, the chemical changes were detected by Fourier transform infrared spectroscopy and differential scanning calorimetry. The crosslink density changes during aging of BEE were determined as well. A plausible aging mechanism of BEE was proposed. It can be concluded that the thermal oxidation process gives priority to further crosslinking in the initial period of aging. As the aging time increases, chain scission becomes the dominant element in the subsequent thermal oxidation process. © 2014 Wiley Periodicals, Inc. J. Appl. Polym. Sci. **2014**, *131*, 40862.

KEYWORDS: ageing; biopolymers and renewable polymers; elastomers

Received 19 November 2013; accepted 14 April 2014
DOI: 10.1002/app.40862

INTRODUCTION

Elastomers play an important role in our daily life. However, most synthetic elastomers are petroleum-based. It is important to explore alternative renewable elastomers to meet the requirements of environmental protection and sustainable development. Bio-based elastomers from renewable resources have received considerable interests from academia and industry in recent years[1,2] as a major alternative to conventional petroleum-based elastomers,[3–8] and will provide a solution to the environmental problem of plastic wastes.[9] The previous bio-based elastomers are basically used as medical materials and most of them are thermosetting elastomers. Thus, it is of vital importance to prepare bio-based elastomer which can be used in engineering applications. As a result, various bio-based elastomers that are both processable and crosslinkable were designed and synthesized to meet the engineering applications. Wang et al. synthesized novel soybean-oil-based elastomers with favorable processability and tunable properties.[10,11] A novel crosslinkable bio-based poly(diisoamyl itaconate-*co*-isoprene) (PDII) elastomer was prepared by emulsion polymerization.[12,13] Wei et al. prepared a novel bio-based engineering polyester elastomer (BEE) by polymerizing commercial biobased monomers—sebacic acid, itaconic acid, succinic acid, propanediol, and butanediol.[14] BEE exhibits low glass transition temperature (T_g), satisfactory elasticity, good mechanical strength, good airtightness, and good environmental stability.

In outdoor applications, the surface properties and service lifetime of elastomers are easily influenced and deteriorated by the weathering conditions, such as light, heat, irradiation, and chemical media, so it is essential to investigate the aging of rubber in such conditions. Many studies have been done on the aging behavior of elastomers, including polyesters, showing that the aging behavior of polyesters is always affected by temperature and oxygen in natural aging and thermal oxidizing aging. The structural changes in the thermal aging of elastomers are attributed to the thermal oxidation process, which includes chain scission and further crosslinking. Rubber usually becomes soft and sticky after aging if chain scission predominates. On the contrary, when crosslinking is the dominant element in the thermal oxidation process, leads to hard and brittle rubber. Both reactions lead to the loss or degradation of the physical properties of the aged rubber.[14–18]

Aging property is an important factor to affect the service life of rubber. As novel bio-based engineering polyester elastomer nanocomposites, the aging properties of BEE nanocomposite

© 2014 Wiley Periodicals, Inc.

was studied. In this work, we prepared bio-based polyester elastomer nanocomposite by mixing bio-based engineering polyester elastomer with carbon. BEE, whose repeat units are based on saturated ester groups, has potentially good thermal stability.[15] Therefore, BEE nanocomposite is expected to perform well in long-term outdoor applications. The mechanical properties of the elastomer and the mechanism of thermal aging were investigated. A plausible aging mechanism was proposed based on results of Fourier transform infrared (FTIR) spectroscopy, differential scanning calorimetry (DSC), thermogravimetric analysis (TGA) and crosslink density measurements.

EXPERIMENTAL

Raw Materials

1,3-propanediol (PDO) (purity 99.0%), and 1,4-butanediol (BDO) (purity 99.0%) were purchased from Alfa Aesar. Itaconic acid (IA) (purity 99.0%), succinic acid (SA) (purity 99.0%), sebacic acid (SeA) (purity 99.0%) were obtained from Guangfu Fine Chemical Institute of Tianjin. Tetrabutyl orthotitanate (TBOT), hydroquinone, and phosphorous acid were supplied by Fluka, Beijing Yili Fine Chenical Co., Ltd, and Sinopharm Chemical Reagent Co., Ltd, respectively. Carbon black N330 (CB N330) was supplied by Qingdao Degussa co., Ltd. Dicumyl peroxide (DCP) was purchased from Fangqian Technology Co., Ltd.

Synthesis of BEE

Our bioelastomer (BEE) was synthesized according to the procedure detailed in our previous work.[14] In brief, we charged PDO (12.54 g, 0.165 mol), BDO (14.85 g, 0.165 mol), SA (15.04 g, 0.1275 mol), IA (5.85 g, 0.04 5 mol), SeA (25.76 g, 0.1275 mol), and the inhibitors hydroquinone (0.0296 g) and phosphorous acid (0.0 074 g) into a 100-mL three-neck flask. The mixture was purged with nitrogen and then heated at 180°C for 2 h. During the reaction, the water formed was distilled off. Then, TBOT (0.05 wt % relative to the quantity of all reactants) was added as the catalyst, and the mixture was heated to 220°C under reduced pressure (<300 Pa) for 3–4 h until the Weisenberg effect was observed. The product BEE was found to have a weight-average molecular weight of ~181,000 g/mol and a polydispersity index of 3.7 by GPC analysis and a glass transition temperature of −56°C by DSC analysis.

Sample Preparation

The CB/BEE compounds were prepared by mixing BEE with 40 phr of CB N330 and 0.16 phr of DCP for 50 min by using a Haake mixer (Rheomix 600p, Thermal Electron Co., USA) at 50°C and a rotational speed of 40 rpm. All the compounds were finally vulcanized under 15 MPa at 160°C for 18 min to produce 2-mm thick sheets.

Characterization

Mechanical Analysis. The dumbbell-shaped samples (25 mm × 6 mm × 2 mm) were prepared according to ISO/DIS 37−1990. The mechanical properties of all vulcanizates were measured at room temperature according to ASTM D624 by a CMT4104 electronic tensile tester (SANS, China) at a crosshead speed of 500 mm/min. At least five specimens were tested for an average value.

Crosslink Density Analysis. The BEE samples were soaked in methylbenzene and removed at regular time intervals, dried superficially with filter paper, weighed, and placed back in the same liquid. Measurements were continued until a constant weight was reached for each sample.

The crosslink density (v_e) was estimated by using a swelling test in *n*-heptane together with the Flory–Rehner equation.[19] The Flory–Rehner equation, as derived from rubber elasticity theory, is shown in the following formula:

$$v_e = \frac{[\chi v_r + \ln(1-v_r) + v_r]}{V_0(0.5v_r - v_r^{1/3})}$$

where v_r is the equilibrium volume fraction of rubber in the swollen state, χ is the polymer–solvent interaction parameter, and V_0 is the molar volume of the solvent. Since the interaction parameter for BEE was unavailable, we used the interaction parameter for acrylic ester as a substitute.

The values of v_r were determined by the following equation:

$$v_r = \frac{1}{1 + \frac{dr}{ds}\left(\frac{1-f_{sol}}{1-f_{sol}-f_{fil}}\right)\left(\frac{W_s}{W_D} - 1\right)}$$

where dr and ds are the densities of the rubber and the solvent, respectively; f_{sol} is the weight fraction of soluble material; f_{fil} is the initial weight fraction of the filler; W_s is the weight of the swollen solvent; and W_D is the weight of the dry sample.

FTIR Analysis. FTIR spectra of the samples were recorded on a TENSOR27 (Bruker Optic GMBH, Germany) Fourier transform infrared spectrophotometer equipped with a Smart Orbit diamond attenuated total reflection (ATR) accessory. Interferograms were Fourier transformed by using cosine apodization for optimum linear response. Absorption spectra were acquired at 4 cm^{-1} resolution, and the signal averaged over 32 scans. All spectra were baseline corrected and normalized to the average of the methyl peaks at 1463 cm^{-1}.

DSC Analysis. DSC thermograms of the samples were recorded by using a STARe system DSC1 calorimeter (Mettler-Toledo International Inc., Switzerland). The temperature was first raised to 100°C at 10 °C/min, allowed to stay there for 5 min to eliminate any thermal history and moisture from the sample, and then lowered to −100°C at 10 °C/min. Data were recorded in the temperature range −100 to +80°C at a heating rate of 10 °C/min. The nitrogen flow was 150 mL/min.

TG Analysis. The measurements of sample weight loss were carried out on a STARe system TGA/DSC1 thermogravimeter (Mettler-Toledo International Inc., Switzerland) with a cooling water circulator. The testing was done under a flowing nitrogen atmosphere (20 mL/min). All the samples used in the thermogravimetric measurements were similar in weight (10 ± 1 mg) and heated from 30 to 800°C at a heating rate of 10 °C/min.

RESULTS AND DISCUSSION

Thermal Aging Properties of BEE

The thermal aging resistance of CB/BEE nanocomposites was tested in an aging oven for different aging times and aging temperatures 100, 125, and 150°C. The effects of aging time and

Table I. Thermal Aging Properties of CB/BEE Composites

Aging temperature (°C)/aging time (h)	Tensile Strength (MPa)	Elongation at break (%)	Modulus at 100% elongation (MPa)	Permanent deformation (%)	Hardness (Shore A)
-/0	12.1 ± 0.5	261 ± 11	2.0 ± 0.07	2	63
100/24	13.4 ± 0.3	295 ± 4	2.5 ± 0.09	2	65
100/48	12.4 ± 0.4	279 ± 9	2.7 ± 0.05	2.5	65
100/72	11.3 ± 0.3	238 ± 10	3.0 ± 0.07	2.5	66
125/24	11.8 ± 0.1	208 ± 13	3.5 ± 0.10	2.5	65
125/48	11.2 ± 0.2	205 ± 4	3.6 ± 0.16	2.5	65
125/72	10.9 ± 0.4	204 ± 14	3.8 ± 0.08	3	67
150/24	11.5 ± 0.7	230 ± 6	3.7 ± 0.14	3	66
150/48	9.49 ± 0.5	163 ± 5	5.0 ± 0.17	3	68
150/72	8.99 ± 0.3	150 ± 12	5.4 ± 0.11	3.5	70

temperature on the mechanical properties of CB/BEE nanocomposites are shown in Table I and Figure 1.

It can be seen from Figure 1 that CB/BEE nanocomposites without any antioxidant exhibits excellent anti-aging properties. The mechanical properties of CB/BEE nanocomposites were found to decrease gradually as the aging time and temperature increase in essence. The tensile strength increases slightly in the first few days at 100°C. The tensile strength retention rates at 100°C and 125°C were both above 90% after 72 h. The elongation at break retention rates at 100°C and 125°C were above 90% and above 78%, respectively, after 72 h. Although there is an obvious decrease in tensile strength after the 72 h/150°C aging, the tensile strength and elongation at break retention rates still stayed around 74.3% and 57.5%, respectively. Take Nitrile rubber for an example, its tensile strength and elongation at break retention rates decreased by 62% and 70%, respectively after the 72 h/150°C aging without antioxidant. BEE behaved better than Nitrile rubber.[20] If we set the failure criterion for rubber as an increase in hardness of 15 units and a decrease in elongation at break of 50%, the BEE composites can work continuously up to 150°C for a long time.[21]

The stress–strain curves of CB/BEE nanocomposites after aging at different temperatures for 72 h are shown in Figure 2. The stress at a given elongation increases as the aging temperature increases, meaning the stiffness and the crosslinking density increased during aging.

Thermal Aging Mechanism for Bio-Based Polyester Elastomer

To gain insight into the changes in the CB/BEE nanocomposites during aging, we investigated the aging mechanism. The BEE strips appear hardened with an increase in hardness of 10 units and their tensile strength increases slightly after the initial thermal aging treatment, but the BEE strips appears to turn soft with a decrease in hardness of 14 units with increasing aging time. A rough judgment on the aging mechanism of BEE might be made. However, the aging mechanism of BEE cannot be deduced from changes in appearance alone. The surface chemistry was monitored by FTIR spectroscopy by using the peak area ratio method. We investigated the internal chemical changes by DSC. Based on the FTIR and DSC results, a plausible aging mechanism was proposed. In addition, the crosslink density of

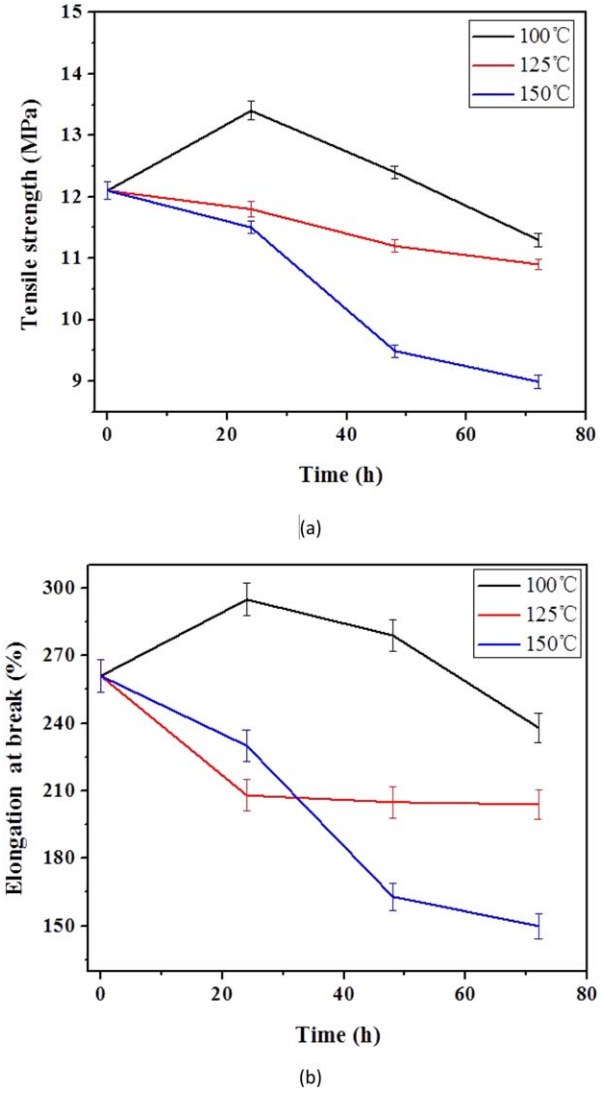

Figure 1. Effects of thermal aging conditions on (a) tensile strength and (b) elongation at break of CB/BEE composites. [Color figure can be viewed in the online issue, which is available at wileyonlinelibrary.com.]

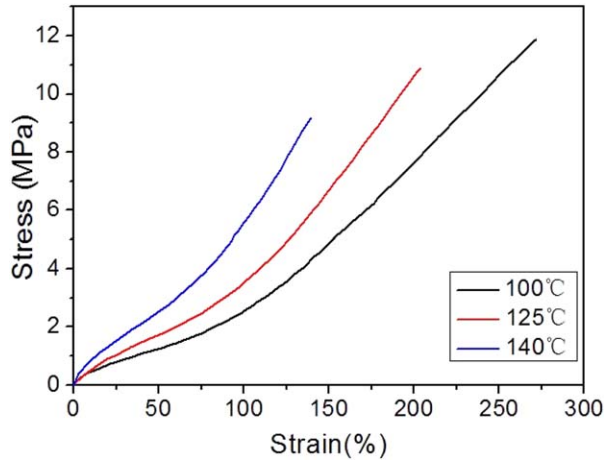

Figure 2. Stress–strain curves of CB/BEE nanocomposites after aging for 72 h at different temperatures. [Color figure can be viewed in the online issue, which is available at wileyonlinelibrary.com.]

CB/BEE nanocomposites was determined by the equilibrium swelling method. Finally, the thermal stability of CB/BEE nanocomposites was evaluated by TGA.

Crosslink Density. The crosslink density of CB/BEE nanocomposites was determined by the equilibrium swelling method. The change in crosslink density of CB/BEE nanocomposites is shown in Figure 3.

Figure 3 shows that the crosslink density of CB/BEE nanocomposites increases from 6.43×10^{-4} to 8.36×10^{-4} mol/cm^3 in the first 10 days of aging and then levels off. After 30 days, the crosslink density begins to decrease slowly, according to the fitted curves. The change of the crosslinking density of CB/BEE nanocomposites indicates that further crosslinking occurs in aging, and the crosslinking rate decreases as the aging time increases.

FTIR. Figure 4(a) shows the FTIR spectra of BEE before and after aging at 100°C, 125°C, and 150°C for 72 h. Both the intense C═O vibration peak at 1736 cm^{-1} and the absorption peak at 1161 cm^{-1} for C—O—C are associated with the existence of ester bonds. The broad absorption peaks at 2932 cm^{-1} and 2857 cm^{-1} are both attributed to the stretching vibration

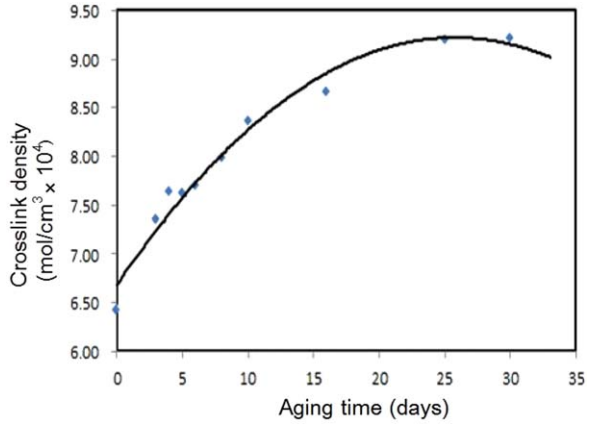

Figure 3. Crosslink density of CB/BEE composite as a function of aging time at 125°C. [Color figure can be viewed in the online issue, which is available at wileyonlinelibrary.com.]

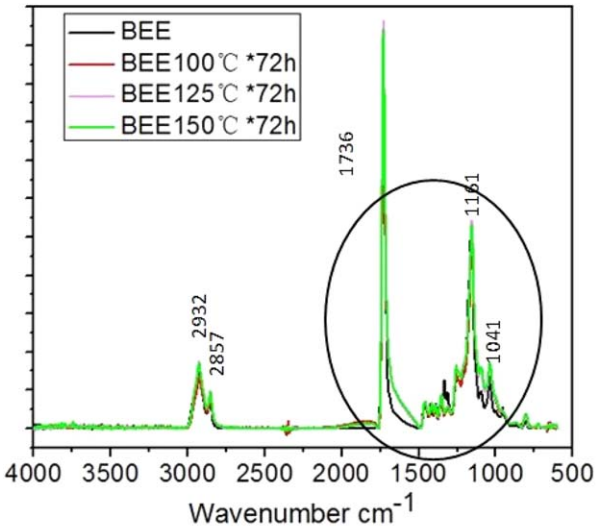

(a)

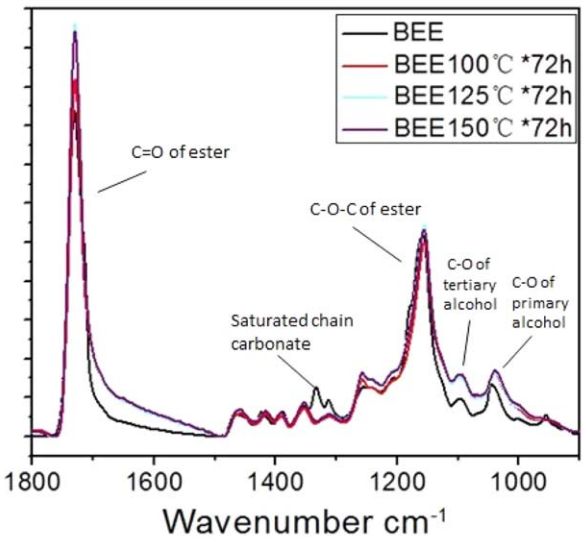

(b)

Figure 4. FTIR spectra of BEE before (a) and after aging (b). [Color figure can be viewed in the online issue, which is available at wileyonlinelibrary.com.]

of —CH_2.The broad absorption peaks at 1045 cm^{-1} and 1098 cm^{-1} are attributed to the C—O bonds of tertiary alcohol and primary alcohol, respectively. The absorption peaks at 1325 cm^{-1} is attributed to saturated chain carbonate. Because the saturated —CH_2 bonds stay relatively constant through the entire aging period, we normalized the FTIR spectrum by using —CH_2 as a reference. The FTIR spectra from 900 cm^{-1} to 1800 cm^{-1} are shown in Figure 4(b). The absorption peak of saturated chain carbonate disappears after aging. But beyond that, no more new absorption peak appears or old peak disappears during aging, but there is a difference between the peak areas before and after aging. We calculated the relative areas of the peaks associated with C═O (1489 cm^{-1} to 1768 cm^{-1}), C—O—C (1201 cm^{-1} to 1130 cm^{-1}, and C—O of both tertiary

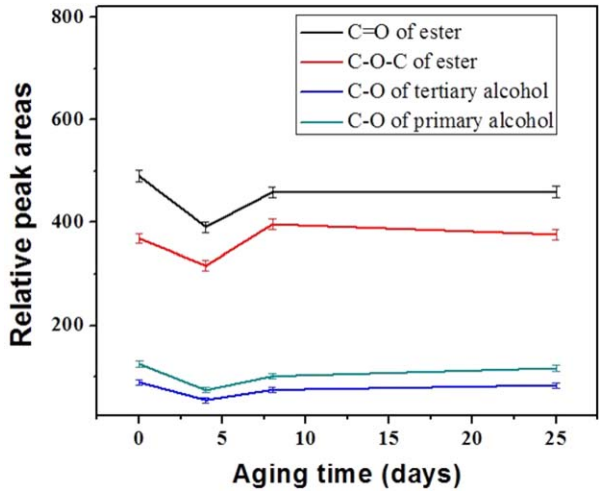

Figure 5. Relative areas of various peaks in FTIR spectra of CB/BEE composite before and after aging at 125°C. [Color figure can be viewed in the online issue, which is available at wileyonlinelibrary.com.]

alcohol and primary alcohol. All these peaks have areas that changed the most during aging. The relative peak area changes of the peaks are shown in Figure 5.

It can be seen from Figure 5 that the relative peak areas of the four kinds of bonds—the C═O bonds, the C—O—C bonds, the C—O bonds in tertiary alcohol, and the C—O bonds in primary alcohol—all first decrease and then increase with increasing aging time. Since there is a positive correlation between peak areas and the number of bonds, the results given in Figure 5 indicate that all four types of bonds first decrease, then increase, and finally level off in number as the aging time increases.

Based on the results of crosslink density and FTIR, a plausible aging mechanism is suggested, as shown in Figure 6. Under the effect of thermal oxidation, peroxy radicals ROO• are formed. These ROO• radicals react with BEE to form hydroperoxides ROOH and alkyl radicals R•. These hydroperoxides decompose into alkoxy radicals RO• and hydroxyl radicals •OH, which can react with BEE to produce alkyl radicals R• and water. The alkyl radicals R• further react with oxygen to form peroxy radicals ROO•, the cyclic process is thus completed. The alkoxy radical RO• is the most important intermediate and can produce various oxygenated species such as ether, ester, and β-diketone. Therefore, it can be concluded that in chain scission, the C—O—C and C═O groups are the main products, accompanied by a small amount of O—C═O.[22]

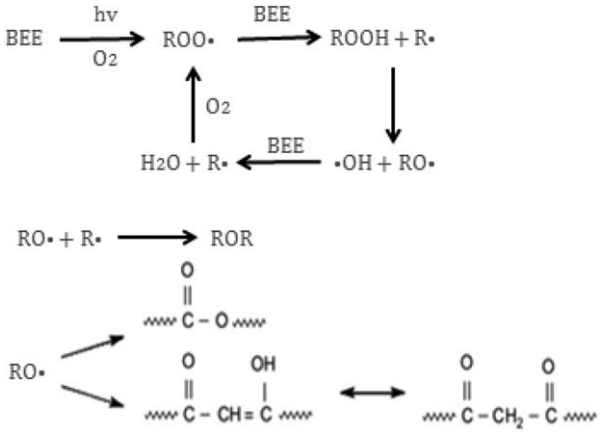

Figure 6. Aging mechanism of BEE.

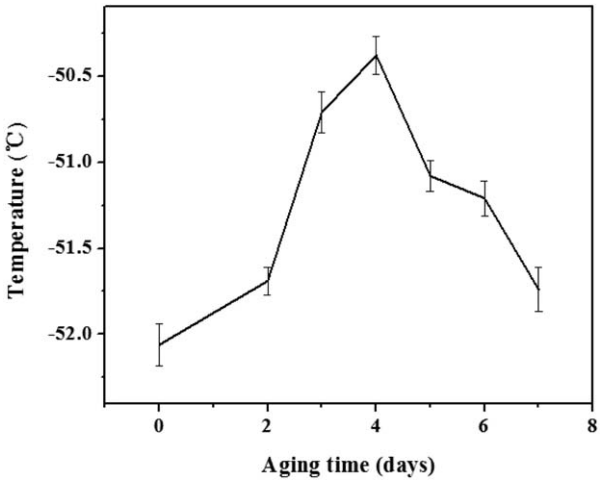

Figure 7. TGA results of CB/BEE nanocomposite before and after aging.

During aging, the saturated chain carbonate of BEE is consumed in the thermal oxidation process. The decrease of four types of bonds mentioned above might be due to further crosslinking and the thermal oxidation process of the molecular chain degradation might then result to the increase latter.

The changes in the number of bonds illustrate that in the first period of aging, crosslinking is the main chemical reaction in the aging of BEE, accompanied by the initial degradation of the BEE molecular chain. The overall mechanical properties are at the enhanced stage, in keeping with the mechanical property changes of BEE. With the increasing aging time, the degradation of the BEE molecular chain gradually becomes more significant, according to FTIR and crosslink density results.

DSC. Since the glass transition temperature is a macroscopic expression of molecular chain movement, the thermal properties and aging mechanisms of CB/BEE nanocomposites can be investigated by considering the changes of T_g during aging. The main factors affecting the properties during aging have been identified by variation of T_g.[23,24] We tracked the change in glass transition temperature of CB/BEE nanocomposites with aging time by means of DSC and the results are shown in Figure 7.

It can be seen that the T_g of CB/BEE nanocomposites reaches a maximum of −50.38°C after 4 days of aging. Since the increase of T_g is attributed to crosslinking and the decrease of T_g is attributed to molecular chain degradation, it can be deduced that the thermal oxidation process gives priority to further crosslinking in the initial period of aging and chain scission is the dominant element later in the thermal oxidation process. This deduction is consistent with the FTIR and crosslink density results.

TGA. The TGA curves of CB/BEE nanocomposites before and after aging are shown in Figure 8. It can be seen that the weight loss and the onset temperature for weight loss both increase with increasing aging time. These results suggest that molecular

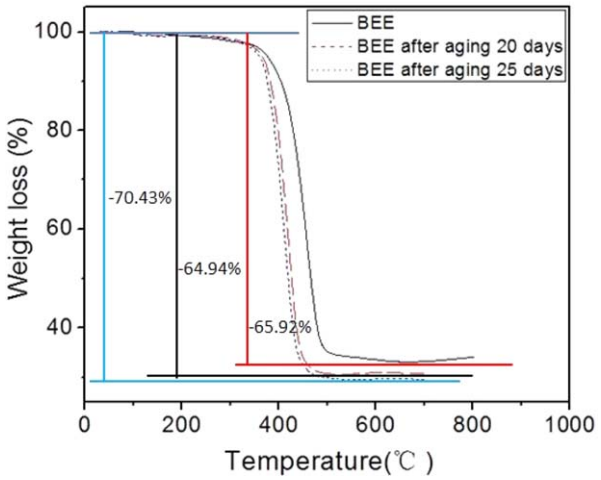

Figure 8. Variation of glass transition temperature of CB/BEE nanocomposite with aging time. [Color figure can be viewed in the online issue, which is available at wileyonlinelibrary.com.]

chain degradation occurs after aging. Since the changes in weight loss are small, we believe that aging does not significantly affect the thermal stability of BEE.

CONCLUSION

Novel bio-based polyester elastomers/carbon (CB/BEE) nanocomposites showed good thermal aging resistance. The mechanical properties of CB/BEE nanocomposites were found to decrease gradually as the aging temperature and time increase. The mechanical property retention rates at 100°C and 125°C were above 90%. The elongation at break retention rates of CB/BEE nanocomposites at 100°C and 125°C for 72 h were above 90% and above 78%, respectively. Although there was an obvious decrease in tensile strength after the aging at 150°C for 72 h, the tensile strength and elongation at break retention rates were still about 74.3% and 57.5%, respectively.

The aging mechanism of CB/BEE nanocomposites at high temperatures was studied for the first time. It can be deduced that the thermal oxidation process in aging gives priority to further crosslinking in the initial period, with an increase in crosslink density and T_g and a decrease of oxygenated species such as C═O, C─O─C and alcohol C─O groups. Chain scission becomes the dominant element in the following thermal oxidation process with the increasing of aging time, which leads to a decrease of T_g and mechanical properties and a increase of oxygenated species. The thermal aging does not affect the thermal stability of BEE significantly.

ACKNOWLEDGMENTS

This work was supported by the National Natural Science Foundation of China (50933001, 51221102).

REFERENCES

1. Dam, J. V.; Junginger, M.; Faaij, A.; Jürgens, I.; Best, G.; Fritsche, U. *Biomass Bioenerg.* **2008**, *32*, 749.
2. Chiellini, E.; Cinelli, P.; Chiellini, F.; Iman, S. H. *Macromol. Biosci.* **2004**, *4*, 218.
3. Wang, Y.; Ameer, G. A.; Sheppard, B. J.; Langer, R. *Nat. Biotechnol.* **2002**, *20*, 602.
4. Amsden, B.; Wang, S.; Wyss, U. *Biomacromolecules* **2004**, *5*, 1399.
5. Yang, J.; Webb, A. R.; Ameer, G. A. *Adv. Mater.* **2004**, *16*, 511.
6. Nijst, C. L.; Bruggeman, J. P.; Karp, J. M.; Ferreira, L.; Zumbuehl, A.; Bettinger, C. J.; Langer, R. *Biomacromolecules* **2007**, *8*, 3067.
7. Bettinger, C. J.; Bruggeman, J. P.; Borenstein, J. T.; Langer, R. S. *Biomaterials* **2008**, *29*, 2315.
8. Ifkovits, J. L.; Padera, R. F.; Burdick, J. A. *Biomed. Mater.* **2008**, *3*, 034104.
9. Williams, C. K.; Hillmyer, M. A. *Polym. Rev.* **2008**, *48*, 1.
10. Wang, R.; Ma, J.; Zhou, X.; Wang, Z.; Kang, H. *Macromolecules* **2012**, *45*, 6830.
11. Wang, R.; Yao, H.; Lei, W.; Zhou, X.; Zhang, L. *J. Appl. Polym. Sci.* **2013**, *129*, 1546.
12. Wang, Z.; Zhang, X.; Wang, R.; Kang, H.; Zhang, L. *Macromolecules* **2012**, *45*, 9010.
13. Wang, Z.; Han, Y.; Zhang, X.; Huang, Z.; Zhang, L. *J. Appl. Polym. Sci.*, **2013**, *10*, 1002.
14. Wei, T.; Lei, L. J.; Kang, H. L.; Qiao, B.; Wang, Z.; Zhang, L. Q.; Coates, P.; Hua, K. C.; Kulig, J. *Adv. Eng. Mater.* **2012**, *14*, 112.
15. Zhao, Q.; Li, X.; Gao, J. *Polym. Degrad. Stab.* **2009**, *94*, 339.
16. Chu, Z.; Feng, Y.; Sun, H.; Li, Z.; Song, X.; Han, Y.; Wang, H. *Soft Matter* **2011**, *7*, 4485.
17. Brice, G.; Cedric, L.; Francoise, L. *J. Phys. Chem. B* **2011**, *115*, 12392.
18. Gulseher, S.; Zhou, Y.; Lee, L.; Wang, S.; Zhang, Y. *J. Phys. Chem. B* **2012**, *116*, 12199.
19. Alberto, B.; Giovanni, P.; Giuseppe, G. *J. Appl. Polym. Sci.* **2011**, *1*, 2904.
20. Su, Z.; Qin, R.; Zhu, H.; Huang, Y. *Silicone Mater.* **2012**, *26*, 248.
21. Zhu, L.; Huang, H.; Zhao, B. *JAM* **2007**, *27*,
22. Li, L.; Greg, M. *ACS Appl. Mater. Interface*, **2013**, *10*, 1021.
23. Lin, Y.; Chen, C. X. *Polymer* **2005**, *46*, 11994.
24. Papanicolaou, G. *J. Appl. Polym. Sci.* **2006**, *99*, 1328.